AD-A044 682 RCA LABS PRINCETON N J F/G 11/1
BASIC ADHESION MECHANISMS IN THICK AND THIN FILMS.(U)
JUL 77 K R BUBE, T T HITCH N00019-77-C-0176
UNCLASSIFIED PRRL-77-CR-29 NL

1 OF 1
ADA044682

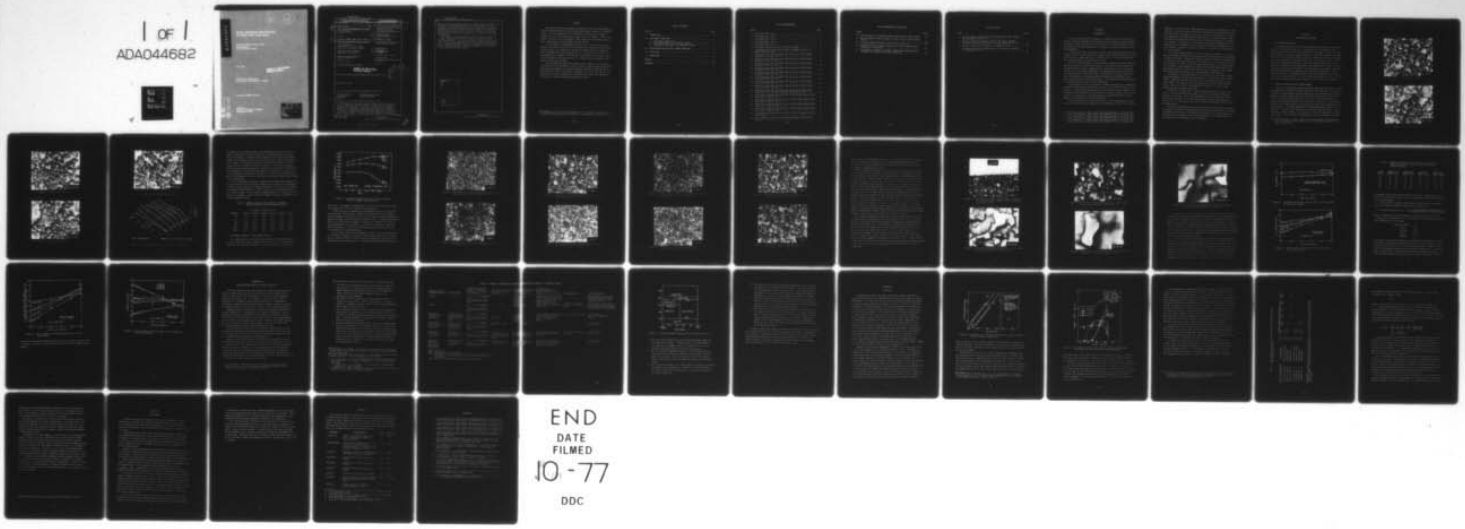

END
DATE FILMED
10-77
DDC

BASIC ADHESION MECHANISMS IN THICK AND THIN FILMS

Kenneth R. Bube and Thomas T. Hitch
RCA Laboratories
Princeton, New Jersey 08540

JULY 1977

QUARTERLY REPORT NO. 2
For the period 1 April 1977 to 30 June 1977

Contract No. N00019-77-C-0176

Prepared for
NAVAL AIR SYSTEMS COMMAND
Washington, DC 20361

UNCLASSIFIED

SECURITY CLASSIFICATION OF THIS PAGE (When Data Entered)

REPORT DOCUMENTATION PAGE

READ INSTRUCTIONS BEFORE COMPLETING FORM

1. REPORT NUMBER: Quarterly rept. no. 2	2. GOVT ACCESSION NO.
3. RECIPIENT'S CATALOG NUMBER	1 Apr - 30 Jun 77
4. TITLE (and Subtitle): BASIC ADHESION MECHANISMS IN THICK AND THIN FILMS	5. TYPE OF REPORT & PERIOD COVERED: Quarterly No. 2 (4-1-77 to 6-30-77)
	6. PERFORMING ORG. REPORT NUMBER: PRRL-77-CR-29
7. AUTHOR(s): Kenneth R. Bube and Thomas T. Hitch	8. CONTRACT OR GRANT NUMBER(s): N00019-77-C-0176
9. PERFORMING ORGANIZATION NAME AND ADDRESS: RCA Laboratories, Princeton, New Jersey 08540	10. PROGRAM ELEMENT, PROJECT, TASK AREA & WORK UNIT NUMBERS
11. CONTROLLING OFFICE NAME AND ADDRESS: Naval Air Systems Command, Washington, DC 20361	12. REPORT DATE: July 1977
	13. NUMBER OF PAGES: 43
14. MONITORING AGENCY NAME & ADDRESS (if different from Controlling Office): 42 Pp.	15. SECURITY CLASS. (of this report): Unclassified
	15a. DECLASSIFICATION/DOWNGRADING SCHEDULE: N/A

16. DISTRIBUTION STATEMENT (of this Report)

APPROVED FOR PUBLIC RELEASE: DISTRIBUTION UNLIMITED

17. DISTRIBUTION STATEMENT (of the abstract entered in Block 20, if different from Report)

18. SUPPLEMENTARY NOTES

19. KEY WORDS (Continue on reverse side if necessary and identify by block number)

Sintering theory
Gold powder
Spinels
Liquid-phase sintering
Reactive bonding

20. ABSTRACT (Continue on reverse side if necessary and identify by block number)

This report is the second quarterly report of the fourth in a series of one-year contracts at RCA to study adhesion mechanisms in thick-film conductors. During this quarter, the sintering kinetics of a specially precipitated gold powder were examined as a function of compaction force, sintering temperature, and time, as well as glass content. It was found that ultimate gold powder

DD FORM 1 JAN 73 1473

UNCLASSIFIED

SECURITY CLASSIFICATION OF THIS PAGE (When Data Entered)

20.

densification was inversely related to powder compaction force. The previously observed retrograde sintering was judged to be due to entrapped air originally present in the compacts before sintering. Conversely, gold powder densification was found to be directly proportional to glass content. This test confirmed that liquid-phase-assisted sintering is operating in at least the first stage of sintering.

With regard to mixed-bonded and reactively bonded conductors, a recent investigation of reaction kinetics and products was critically reviewed. This review served to update and refine the nature and extent of experiments that need to be performed in this area. Proposed experiments include the elucidation of the formation of reaction products and, the relationship of these products to both substrate and metal phases.

PREFACE

This quarterly report describes work performed in the Process and Applied Materials Research Laboratory of RCA Laboratories under Contract No. N00019-77-C-0176. Dr. Paul Rappaport* was the Laboratory Director and Dr. George L. Schnable is the Project Supervisor and Group Head. Dr. Thomas T. Hitch is the Project Scientist and, with Kenneth R. Bube, comprises the principal research team. James Willis is the Government Project Monitor.

It is a pleasure to acknowledge the help of R. J. Paff, who has contributed to this study by his use of x-ray diffraction techniques for phase identification, and to B. Seabury for his work in scanning electron microscopy. We also acknowledge the able assistance of E. J. Conlon and A. Z. Miller in the preparation of samples and in the day-to-day pursuit of this study. Discussions throughout the work with Dr. G. L. Schnable and his reviews of the manuscript were most valuable.

We also acknowledge helpful discussions with a number of the scientists studying thick-film technology in several companies and government laboratories. Discussions with members of the Naval Research Laboratories team working in coordination with RCA, including Dr. Jim Murday, Dr. Paul Becher, and Dr. Bill Bascom; with the Project Monitor, Mr. James Willis; and with his supervisor, Dr. Herbert J. Mueller, have been particularly useful.

*Dr. Rappaport has since left RCA Laboratories for the position of Director, Solar Energy Research Institute, Golden, CO. His successor is Joseph H. Scott.

TABLE OF CONTENTS

LIST OF ILLUSTRATIONS

LIST OF ILLUSTRATIONS (Continued)

LIST OF TABLES

SECTION I

INTRODUCTION

This is the second quarterly report on a contract that is the fourth in a series of one-year programs at RCA, sponsored by the Naval Air Systems Command. The object of the study series has been to improve the understanding of hybrid film materials and, particularly, of the property of adhesion strength in thick-film conductors.

In each of the first three years of study, investigation was confined principally to one or two new classes of conductor inks. Gold conductors were studied in 1974 [1]; copper and silver were added in 1975 [2]; and gold-platinum-type conductors were first studied in 1976 [3].

In each of these studies a broad spectrum of commercial inks was chemically analyzed, printed, and fired with a matrix of processing variations; adhesion strength and other physical properties were then measured on the fired films. Analysis of the ink powder morphology, the bonding phase-to-metal phase interface microstructure in the fired films, and other data allowed classification into three classes: frit-bonded, reactively bonded, and mixed-bonded inks. These classifications relate ink chemistry to the behavior of adhesion strength as influenced particularly by firing temperature.

A second part of each of the contract studies investigated the fundamental properties of materials characteristic of those used in thick-film paste formulations. The wetting and spreading of glass on metal and ceramic surfaces, the sintering of metal powders with or without the presence of glass, and the measurement of the adhesion of the film prepared by innovative methods are only some of the properties that have been measured.

The achievements of the first three years of study have produced a broad base of data on thick-film conductors, their adhesion, and some of the processes

---

1. T. T. Hitch and K. R. Bube, "Basic Adhesion Mechanisms in Thick and Thin Films," Final Report, NASC Contract No. N00019-C-74-0270, 31 January 1975.
2. T. T. Hitch and K. R. Bube, "Basic Adhesion Mechanisms in Thick and Thin Films," Final Report, NASC Contract No. N00019-75-C-0145, 30 January 1976.
3. K. R. Bube and T. T. Hitch, "Basic Adhesion Mechanisms in Thick and Thin Films," Final Report, NASC Contract No. N00019-76-C-0256, 31 January 1977.

important to their behavior. Although most data are more phenomenological than theoretical, several individual inks and certain model film materials have been described rather thoroughly. At RCA, as a result of these studies, the chemical constituents and some physical properties of the conductor pastes, model ink powders, and substrates have been classified and thus related to the adhesion strength. In addition, the theories of sintering and wetting, which are pertinent to the development of film properties in thick-film conductors, have been examined. However, no attempt to predict the properties of ink materials has been attempted.

To test our understanding of thick-film conductor materials, it is desirable to formulate theories for their behavior, which will model the development of adhesion strength. During the firing of thick-film conductors a large number of reactions occur that could affect their adhesion. It is believed to be possible, however, to form a theory that emphasizes the effects of the most important reactions. Even though such a theory will doubtless require the use of adjustable parameters to model film behavior, such an approach can be highly informative and should improve our understanding of these materials.

Accordingly, a major objective of the fourth year in the study of "Basic Adhesion Mechanisms in Thick and Thin Films" is to create models of the development of adhesion strength properties in thick-film conductors and to test those models. The plan calls for the separation of the work into two major parts: first, the study of frit-bonded inks; second, the study of mixed-bonded inks and reactively bonded inks.

Because of the complexity of directly modeling adhesion strength on the basis of the ink characteristics alone, the study of frit-bonded inks will proceed in two steps. One is the development of film microstructure during processing. The other is the modeling of adhesion strength development as a function of the microstructure and of the surface energy between the metal and the binder phase.

The work on mixed-bonded and reactively bonded inks will similarly require a correlation of adhesion strength with microstructures and interfacial energies. In addition, however, for these materials the nature of the binder-phase structures will also be studied. Both the identification of the binder phase and the kinetics of its development will be examined.

SECTION II

FRIT-BONDED CONDUCTORS

A. GOLD POWDER PREPARATION

Five additional 20-g lots of MK-2 gold powder were prepared as described in the first quarterly report [4]. Scanning electron micrographs (SEMs) of powder samples from the five lots, labeled 8-12, are shown in Figs. 1-5. With the exception of occasional large clusters, the individual particles are generally in the 1-2-μm range. Whether clusters or individual particles, the shapes are roughly spherical. This morphological form is believed to result from the rather fast nucleation and growth. Under the conditions used, i.e., rapid addition of concentrated reducing agent, little opportunity is given for slower, anisotropic growth on the relatively faster growing crystal planes. Only one hexagonal-shaped particle, indicative of slower particle growth, is visible in lot 12 (Fig. 5). Subsequently the five lots were combined into one lot by the use of isopropyl alcohol to prevent cold welding between particles, rinsing with methyl alcohol, drying at less than 125°C, and cooling in a dessicator.

B. SINTERING BEHAVIOR OF GOLD POWDER COMPACTS

Because the MK-2 powder exhibited swelling under isothermal (900°C) sintering conditions, as shown in the last quarter, it was necessary to determine the cause prior to undertaking sintering comparisons with glass added to the gold. Samples of the MK-2 powder weighing 0.85 g were compacted in a carbide die of 0.5-in. (12.5-mm) diameter, as usual, at a force of 1900 lb (864 kg), and heated isothermally at 400-900°C for time periods of 30-2400 s. The diametral swelling of the sample shown in Fig. 6 occurs at 600°C after isothermally heating for 2400 s. At higher temperatures the swelling becomes evident in less than 600 s. When the sintering data are expressed as percent change in actual density, as shown in Table 1, the swelling at the higher temperatures becomes more evident. Since foreign contaminants were kept to a minimum in preparing

4. T. T. Hitch and K. R. Bube, "Basic Adhesion Mechanisms in Thick and Thin Films," Quarterly Technical Report No. 1, NASC Contract No. N00019-77-C-0176, 30 April 1977.

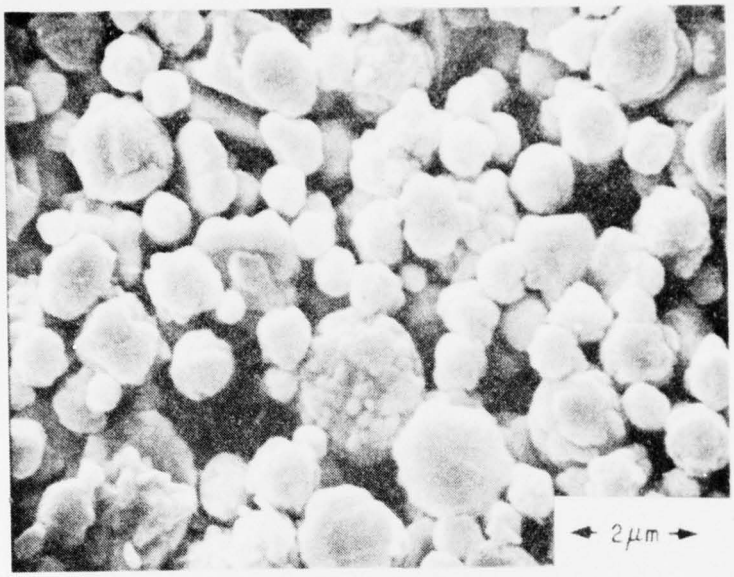

Figure 1. Gold powder MK-2, lot 8.

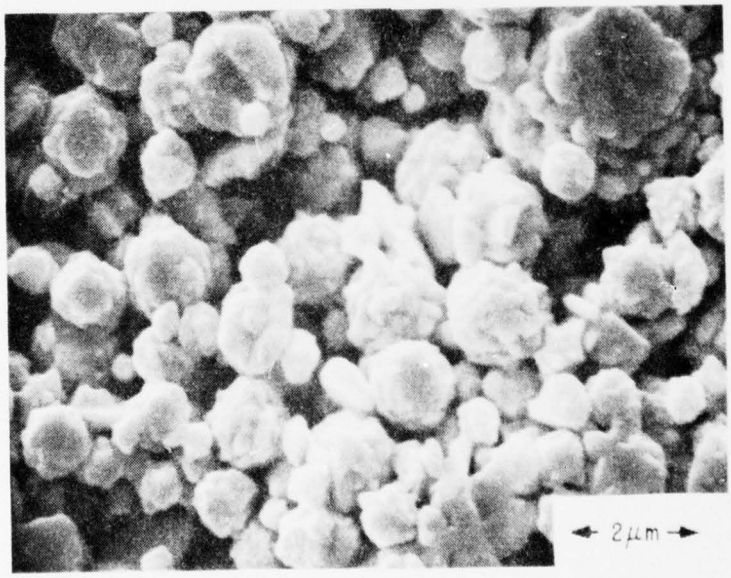

Figure 2. Gold powder MK-2, lot 9.

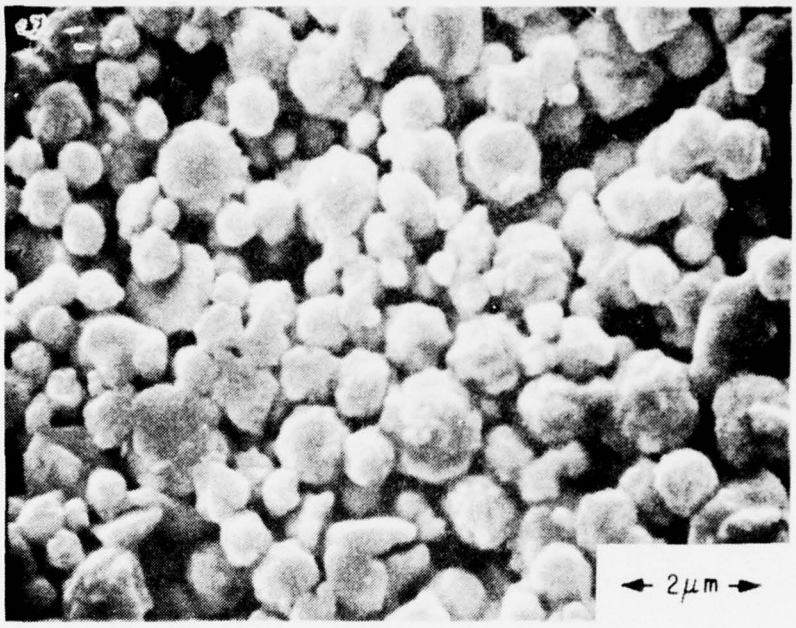

Figure 3. Gold powder MK-2, lot 10.

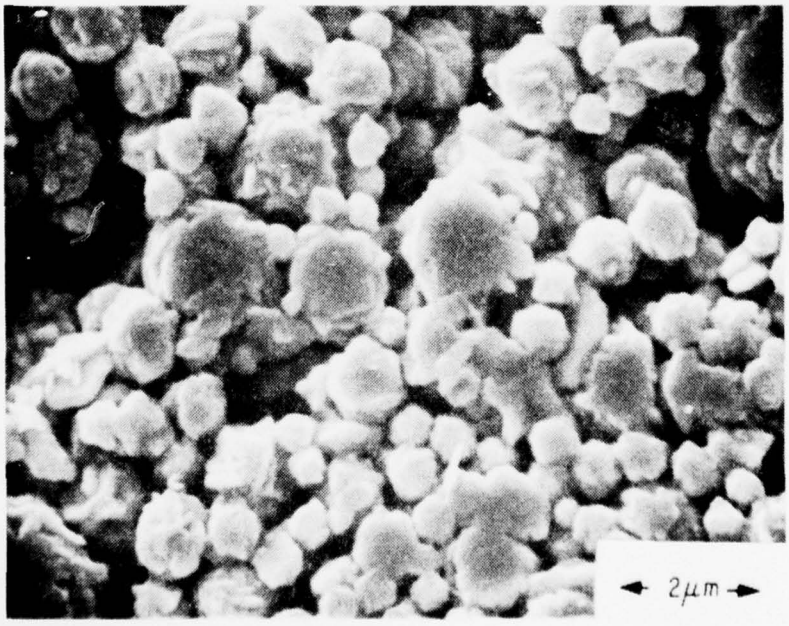

Figure 4. Gold powder MK-2, lot 11.

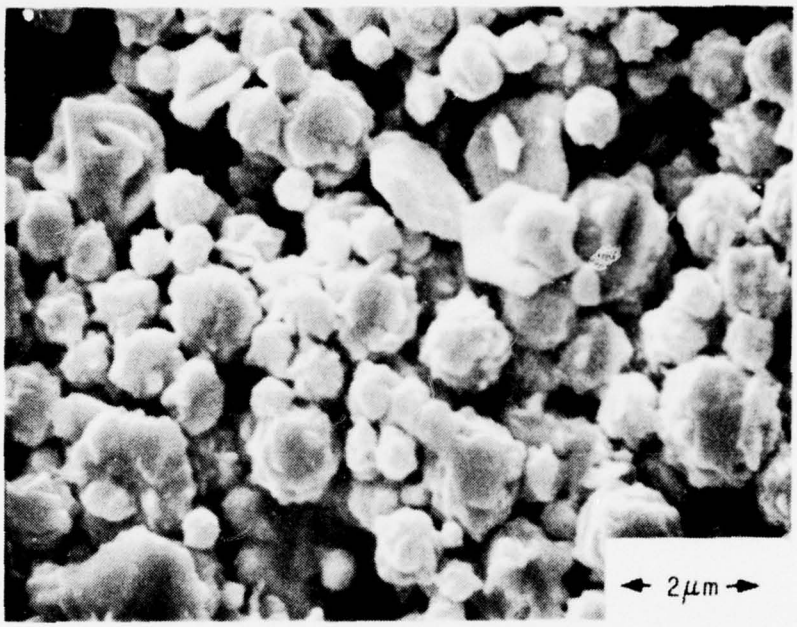

Figure 5. Gold powder MK-2, lot 12.

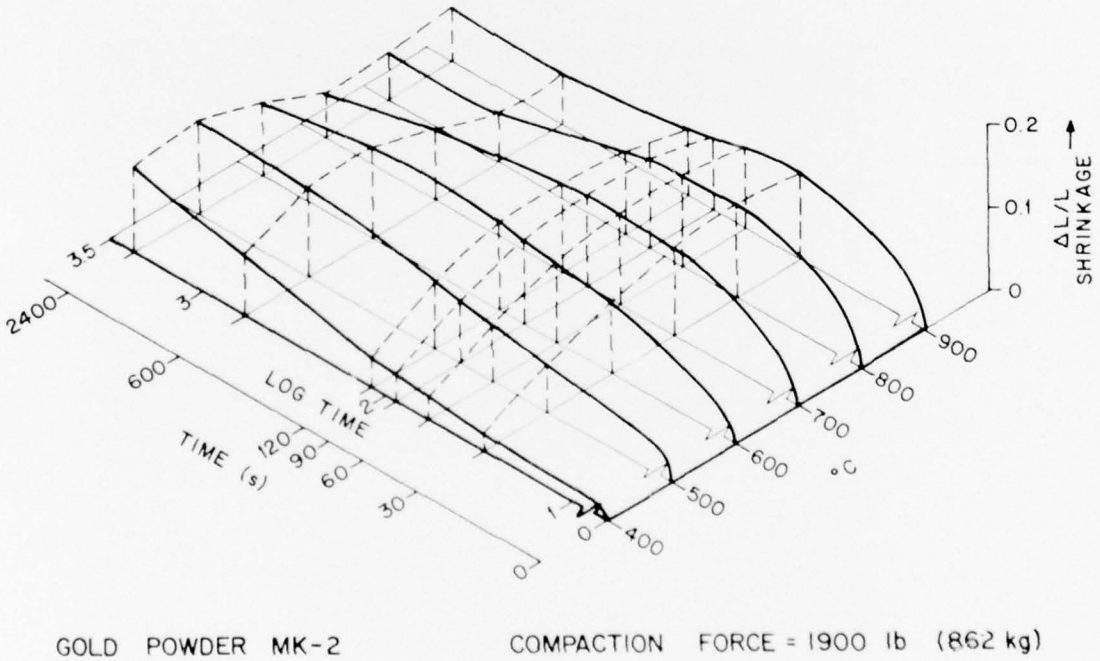

Figure 6. Isothermal densification rates for MK-2 Au powder.

the powder, and the average weight loss on heating was only 0.07 wt pct, it did not seem plausible that the outgassing of adsorbed material could have caused the swelling. A possible cause, however was air sealed in the powder compact by a compaction force that was excessively high. When the temperature of the compact is raised during sintering, the tensile strength of gold decreases, while the trapped-air pressure increases. In an effort to achieve equilibrium, the internal pressure was increased; this resulted in some plastic flow (expansion) of the sintered gold compact. On cooling, the air pressure in the expanded pores decreased. However, the increase in the strength of the gold at room temperature prevents the greater atmospheric pressure from collapsing the sealed pores.

To confirm the above hypothesis, samples of MK-2 powder were compressed at 475 lb (215 kg) and 950 lb (431 kg), respectively, and were fired isothermally at 700°C; at this temperature swelling was observed in the case of the samples compressed at 1900 lb (862 kg). Figure 7 shows that the swelling decreases with compaction force and is virtually eliminated when 475 lb (215 kg) or 2419 lb/in.^{2} (1.7 kg/mm^2) is used. Further experiments therefore utilized the 475 lb (215-kg) compaction force.

TABLE 1. PERCENT CHANGE IN ACTUAL DENSITY OF SINTERED MK-2 GOLD [1900-lb (862 kg) COMPACTION FORCE]

	Pct Change at Temperature (°C)					
Time (s)	400	500	600	700	800	900
30	4.7	7.4	28.6	35.1	36.6	34.5
60	3.2	21.2	30.6	33.5	35.3	30.0
90	8.6	17.3	28.4	33.1	32.7	24.5
120	16.4	26.3	32.8	32.2	32.9	23.8
600	16.4	38.2	35.4	20.9	13.8	16.9
2400	32.6	35.6	26.2	12.9	13.6	20.0

C. GOLD POWDER SINTERING IN THE PRESENCE OF GLASS

Gold powder MK-2 was blended with quantities of E1527 glass necessary to make up individual powder compacts weighing 0.85 g. The blending was accomplished for these small quantities by careful mixing with a spatula on a

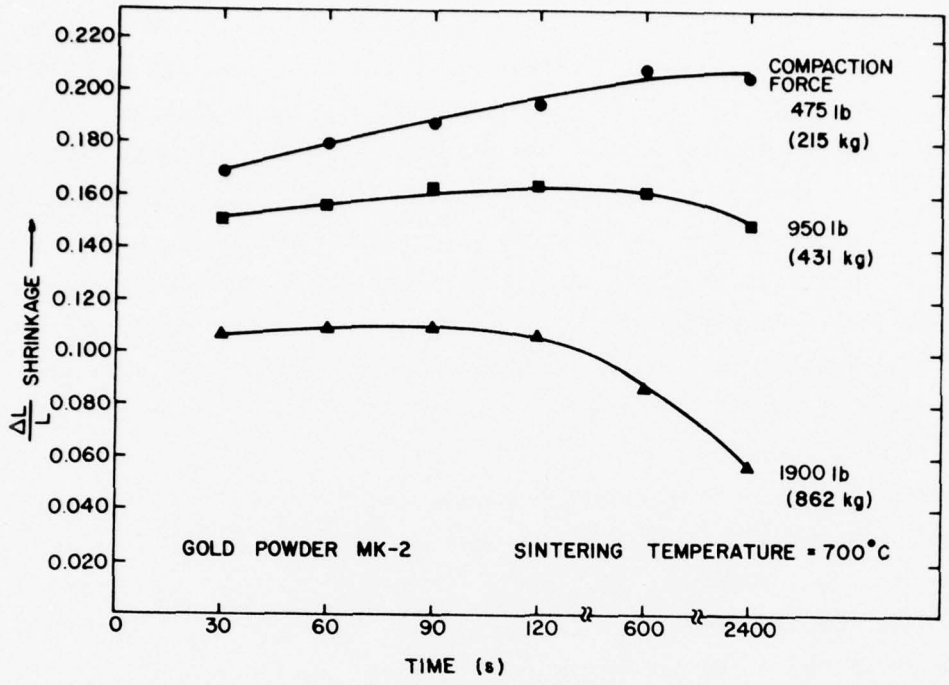

Figure 7. Isothermal densification rates for MK-2 Au powder at 700°C vs powder compaction force.

glass plate. All samples, containing 10, 20, 30, 40, or 50 vol pct of glass were compacted at 475 lb (215 kg) in the usual manner.

During this quarter, samples were isothermally sintered at 700 and 800°C for 30 and 600 s in both cases. Samples of the 700°C-30-s and 700°C-600-s sintered compacts containing 10 and 50 vol pct of glass were metallographically mounted, polished, and etched with aqua regia at 50°C. A similar treatment was given to the 800°C-sintered samples. Figures 8-15 illustrate the degree of phase agglomeration which occurred as a function of temperature, time, and glass concentration. In each case, phase dispersion is uniform, attesting to the adequacy of spatulated-mixing.

At the lowest time (30 s) and temperature (700°C) the glass phase (dark) in the 10-vol pct sample is very finely and uniformly dispersed, as shown in Fig. 8. Heating for 600 s at 700°C produces considerable coarsening in the microstructure, as shown in Fig. 9. The glass becomes isolated into fewer but

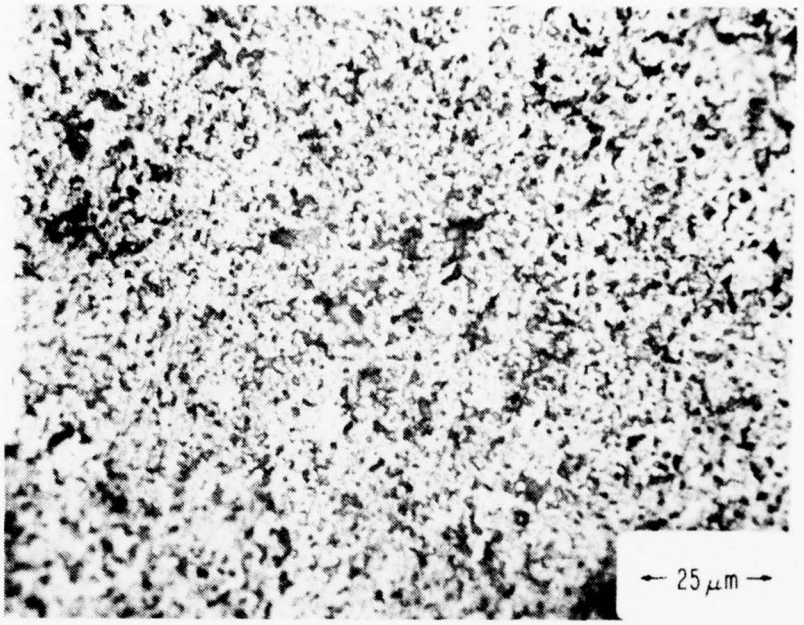

Figure 8. Microstructure of MK-2 Au powder with 10 vol pct of E1527 glass sintered at 700°C for 30 s.

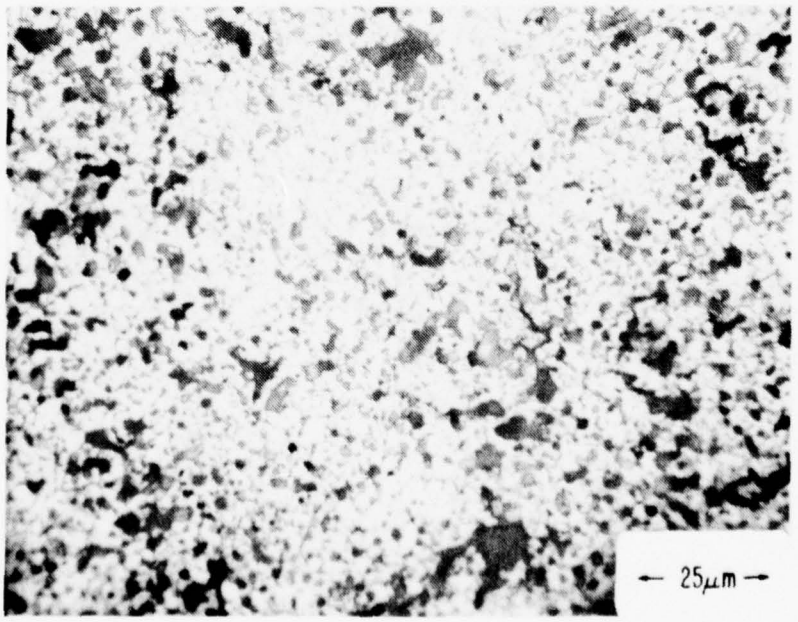

Figure 9. Microstructure of MK-2 Au powder with 10 vol pct of E1527 glass sintered at 700°C for 600 s.

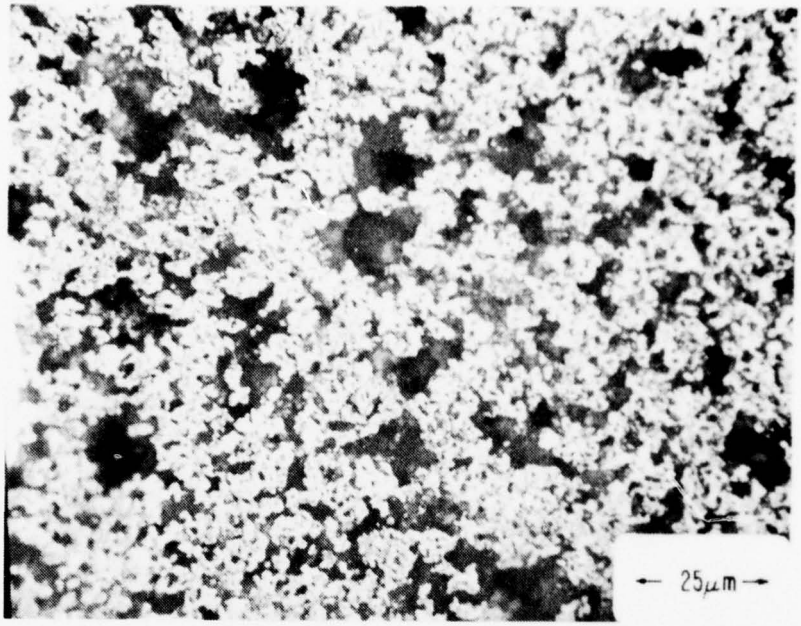

Figure 10. Microstructure of MK-2 Au powder with 50 vol pct of E1527 glass sintered at 700°C for 30 s.

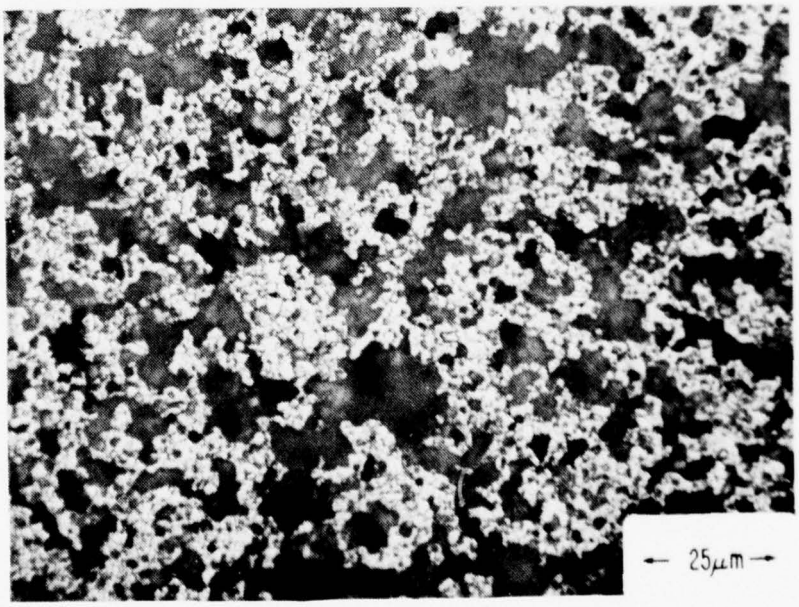

Figure 11. Microstructure of MK-2 Au powder with 50 vol pct of E1527 glass sintered at 700°C for 600 s.

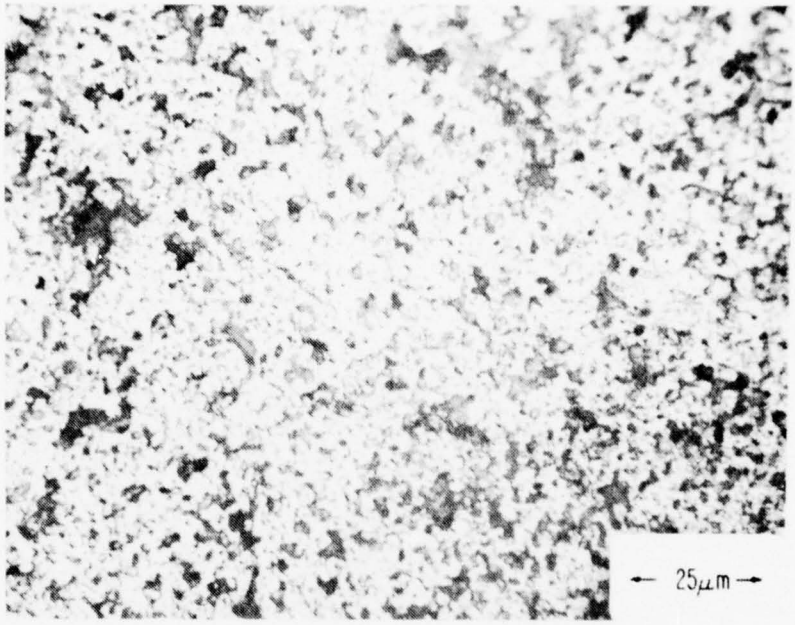

Figure 12. Microstructure of MK-2 Au powder with 10 vol pct of E1527 glass sintered at 800°C for 30 s.

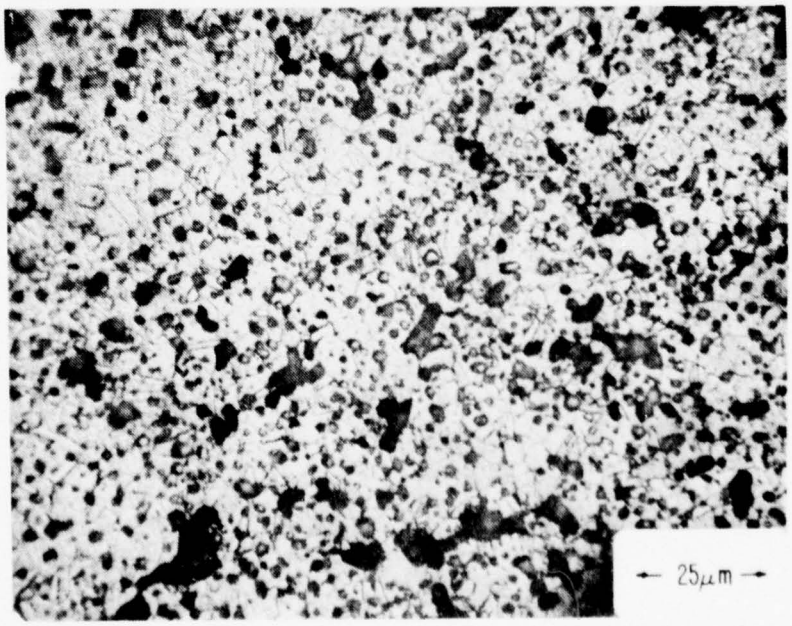

Figure 13. Microstructure of MK-2 Au powder with 10 vol pct of E1527 glass sintered at 800°C for 600 s.

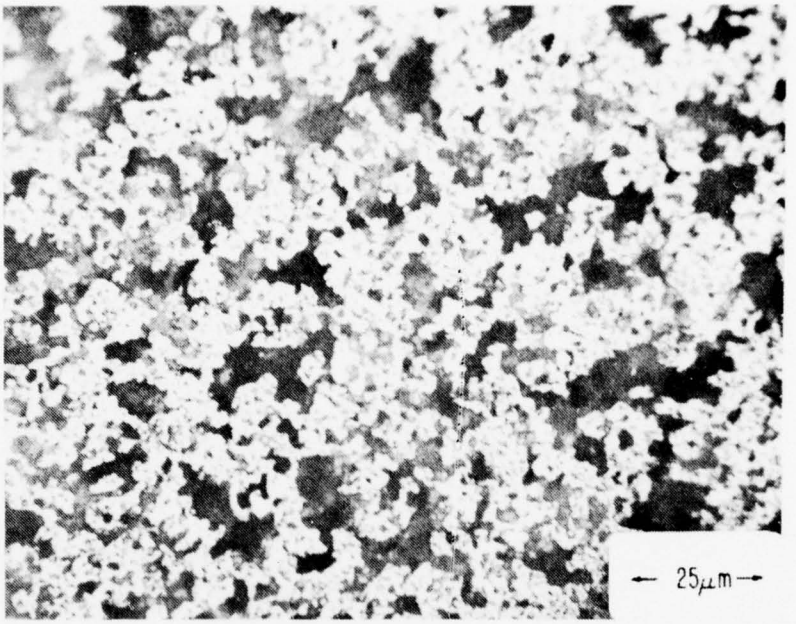

Figure 14. Microstructure of MK-2 Au powder with 50 vol pct of E1527 glass sintered at 800°C for 30 s.

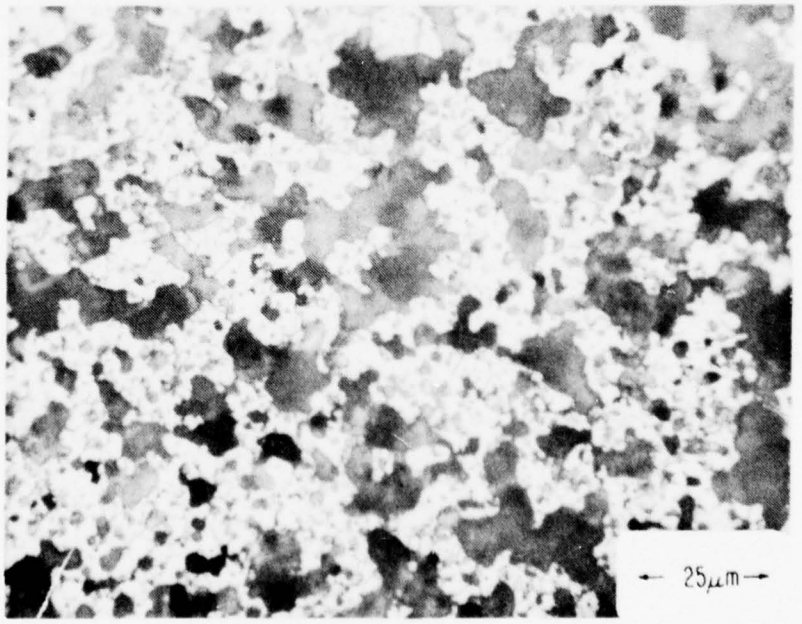

Figure 15. Microstructure of MK-2 Au powder with 50 vol pct of E1527 glass sintered at 800°C for 600 s.

larger pockets as gold sintering progresses. At 50 vol pct, the glass pockets are still adequately dispersed but are correspondingly larger than those in the 10-vol pct samples as shown in Figs. 10 and 11 for the sintering times of 30 and 600 s, respectively, at 700°C.

When the samples containing 10 and 50 vol pct of glass are fired at 800°C, the results differ only in degree (see Figs. 12-15). The dispersion is again quite uniform, but the extent of phase agglomeration is somewhat greater for the 800°C-sintered samples. Compare Figs. 8 and 12 for 30 s, 10 vol pct glass, 9 and 13 for 600 s, 10 vol pct glass, 10 and 14 for 30 s, 50 vol pct glass, and 11 and 15 for 600 s, 50 vol pct glass. Therefore, at temperatures where the glass is fairly fluid (700 and 800°C), i.e., well above its 485°C softening point, the two phases begin to separate with sintering time. As gold particle neck growth occurs, the more fluid glass phase is extruded into the few remaining voids in the structure. Where the glass phase is already isolated from contact with adjacent pores, the glass remains trapped in the sintered gold matrix. However, a sizeable percentage of glass escapes to the outer surface of the sintered gold compact, as can be seen in Fig. 16 in the case of the sample containing 50 vol pct of glass, fired at 800°C for 600 s. It is this interfacial glass layer which enhances adhesion of the gold layer to the ceramic body in screen-printed conductor applications and which also retards subsequent attempts to bond to the free surface of the film after firing.

After photomicrography was completed, the gold compacts were removed from the epoxy mount by dissolving of the epoxy in glacial acetic acid. The glass phase was then removed from the gold compact by immersion in ultrasonically agitated hydrofluoric acid. In this manner, scanning electron microscopy was able to depict the labyrinthian network of interconnecting gold particles. The 10 vol pct glass sample fired at 700°C for 30 s, illustrated in Fig. 17, shows numerous examples of grain growth, the final stage of sintering. Because of a smaller gold volume fraction in the 50 vol pct glass sample shown in Fig. 18, fewer examples of grain growth are obvious. After firing for 600 s at 800°C this distinction is less clear since grain growth is quite well advanced in both the 10 and 50 vol pct glass samples, as shown in Figs. 19 and 20, respectively.

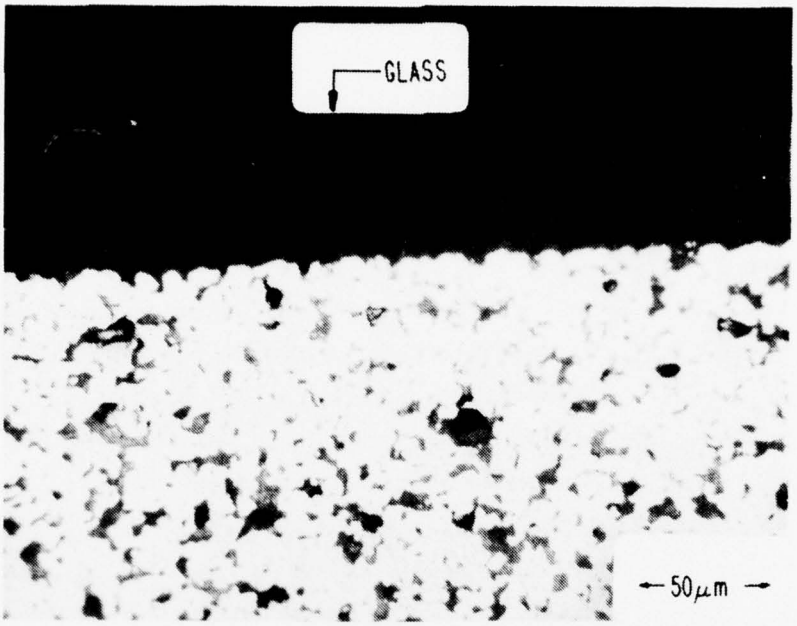

Figure 16. Microstructure of MK-2 Au powder with 50 vol pct of E1527 glass sintered at 800°C for 600 s, showing surface glass layer.

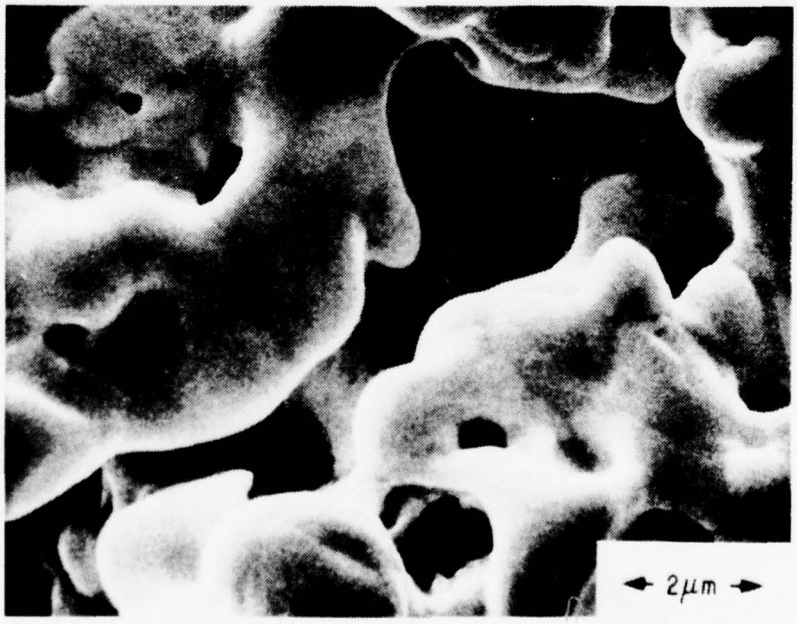

Figure 17. SEM of MK-2 Au powder with 10 vol pct of E1527 glass removed after sintering at 700°C for 30 s.

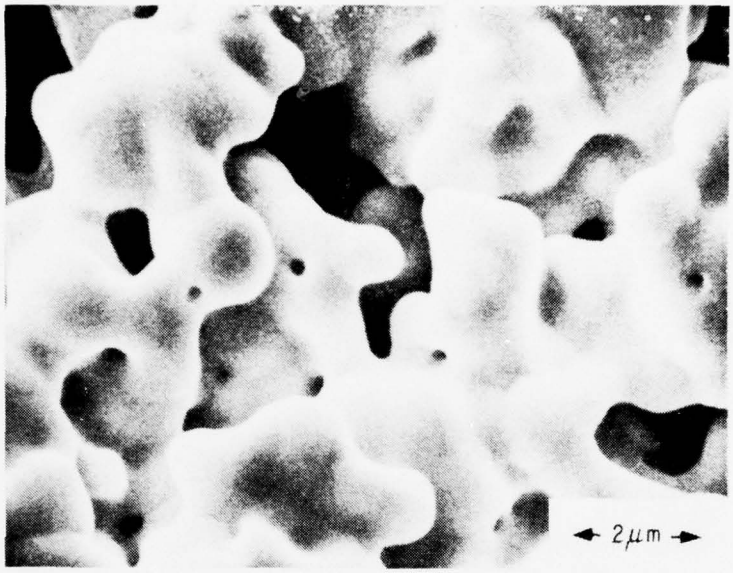

Figure 18. SEM of MK-2 Au powder with 50 vol pct of E1527 glass removed after sintering at 700°C for 30 s.

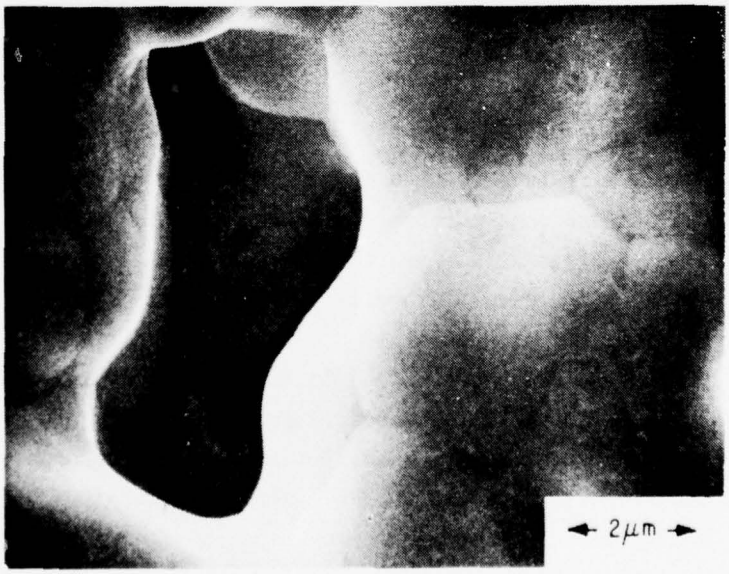

Figure 19. SEM of MK-2 Au powder with 10 vol pct of E1527 glass removed after sintering at 800°C for 600 s.

Figure 20. SEM of MK-2 Au powder with 50 vol pct of E1527 glass removed after sintering at 800°C for 600 s.

To compare the effect of different glass volume fractions on gold densification, two characteristics observed in the system must be recognized. From Fig. 21, which compares $\Delta L/L$ with glass content, it would appear that glass improves densification at 700°C when fired for 30 s, but begins to retard it when fired for 600 s. However, when thickness variations are taken into account so that densities may be compared, a monotonic densification is observed for all samples (see Fig. 22). Apparently powder shrinkage can be anisotropic with regard to direction, i.e., diameter vs thickness. At this time it is not understood why this condition exists.

The second characteristic pertains to the variations in density before sintering as a function of glass content. From Fig. 22 it would appear that increasing glass content enhances densification, since the higher glass contents result in a closer approach to the theoretical density. However, a comparison of powder compact densities *before* sintering, as shown in Table II, indicates that density increases with glass content. Therefore, the glass frit has a sufficient quantity of fine particles to fill some of the voids normally present between some gold particles. Packing efficiency and

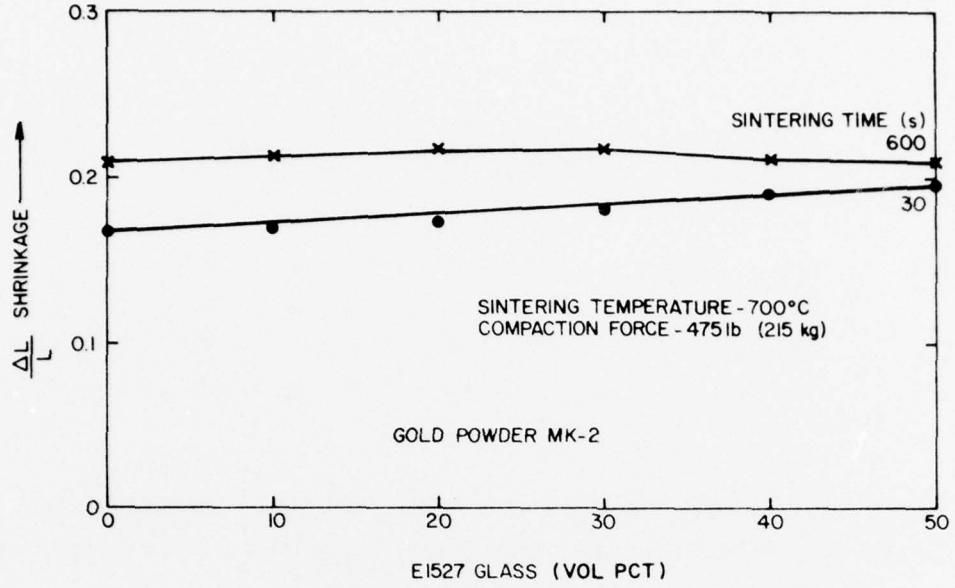

Figure 21. Isothermal densification rate at 700°C for MK-2 Au powder vs E1527 glass content.

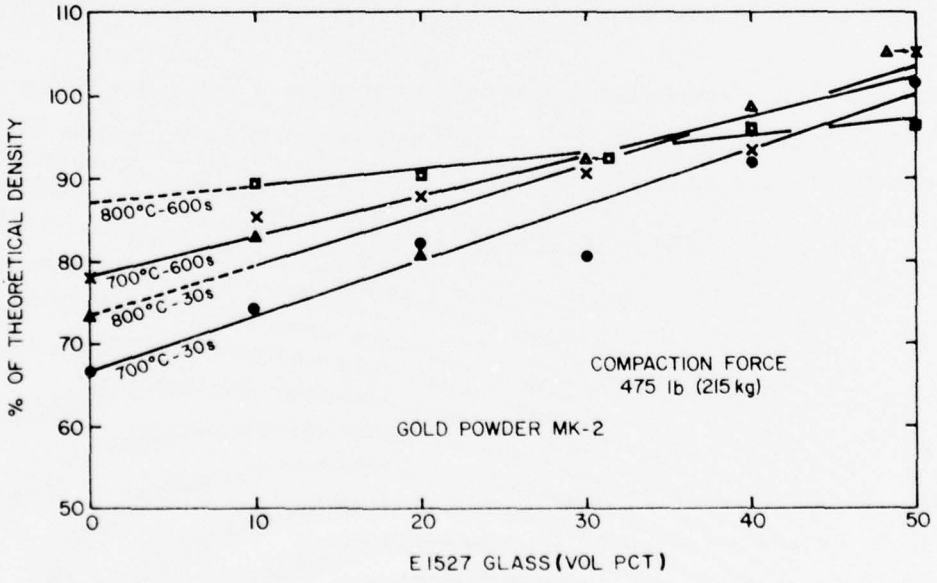

Figure 22. MK-2 Au powder as percent of theoretical density vs E1527 glass content.

TABLE 2. PERCENT OF THEORETICAL DENSITY OF MK-2 GOLD BEFORE AND AFTER SINTERING WITH E1527 GLASS [475-lb (215 kg) COMPACTION FORCE].

Glass Vol Pct	700°C-30 s		700°C-600 s		800°C-30 s		800°C-600 s	
	Before	After	Before	After	Before	After	Before	After
10	44	74	43	85	44	83	39	89
20	46	82	44	88	44	81	44	90
30	48	80	47	90	48	92	47	92
40	50	92	50	93	51	99	51	96
50	56	102	54	105	55	105	55	96

consequently density thus improved with glass content. Superficially, a plot based on the theoretical density gives the appearance of enhanced densification with increasing glass.

A more accurate comparison would account for variations in presintered density by comparing normalized improvements in density, i.e.,

$$\text{Pct normalized densification} = 100\left(\frac{\text{Final density - initial density}}{\text{theoretical density - initial density}}\right)$$

Figure 23 shows this corrected comparison with glass content for which the coefficients of determination, r^2, of the slopes for the respective temperature-time combinations are as follows:

Temp.(°C)-Time(s)	r^2
700-30	0.91
700-600	0.87
800-30	0.91
800-600	0.92

Therefore, it may be safely assumed that densification improvement is directly and linearly proportional to glass volume fraction. Note, however, that the slopes are more positive for the short sintering time (30 s) samples. This implies that sintering during the initial stage of sintering, i.e., rearrangement, is aided more by the presence of glass than during the final stage (600-s-sintered samples) where solid-state processes predominate. The latter

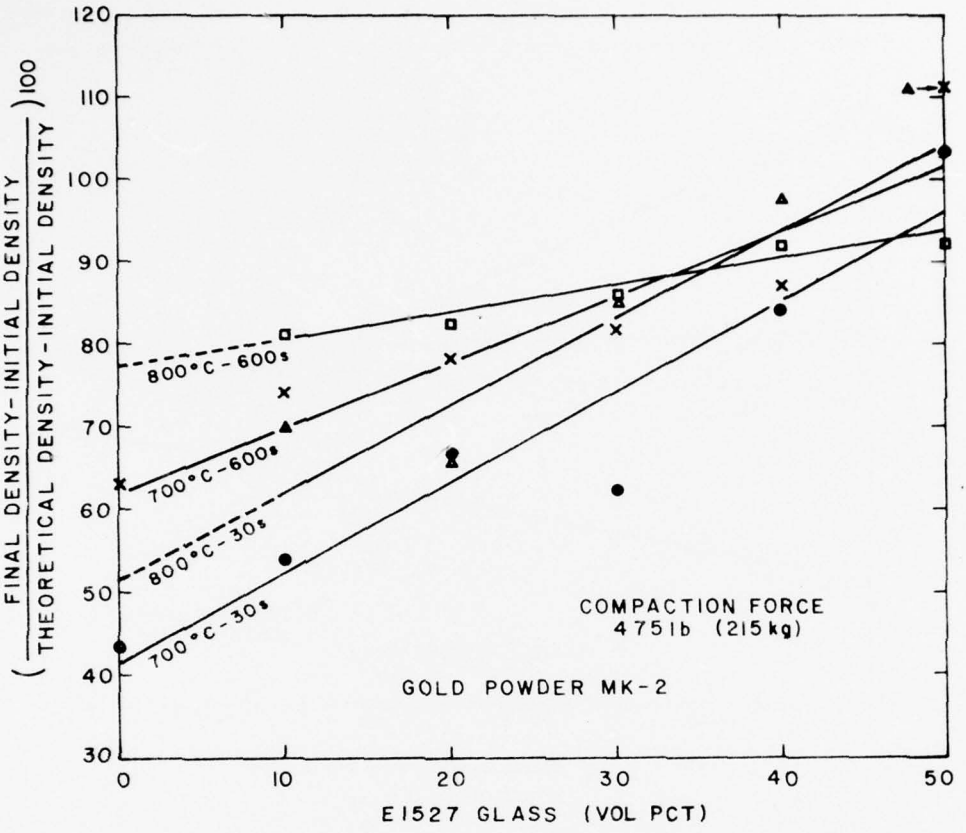

Figure 23. MK-2 Au powder as normalized densification vs E1527 glass content.

observation becomes more vividly apparent when percent change in actual density is compared, as in Fig. 24, where the slopes of 600-s-sintered samples become negative.

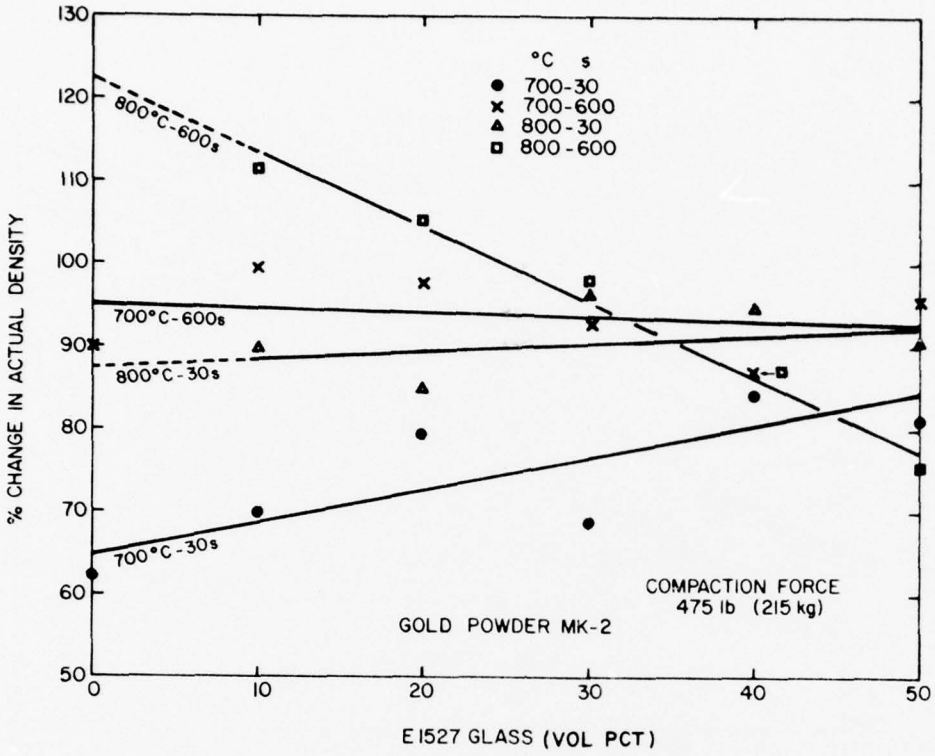

Figure 24. MK-2 Au powder as percent change in actual density vs E1527 glass content.

SECTION III

MIXED-BONDED AND REACTIVELY BONDED CONDUCTORS

In the last quarterly report [4] we briefly reviewed several papers that dealt with spinel formation, reactive bonding, and the pertinence of these effects to the study of thick-film adhesion. Since then another important study has come to light [5]. The findings of this work, an MIT Master's thesis by R. J. Lisauskas, are so directly applicable and complementary to our study of reactively bonded and mixed-bonded conductor adhesion that we are presenting a synopsis of his work here, since it is not generally available.

Lisauskas studied the mechanism of adhesion in gold mixed-bonded and reactively bonded inks. He investigated four commercial materials. The two reactively bonded inks contained Cu and Cd binders in a nominal 3:1 ratio to each other but with differing ratios of binder to gold. The two mixed-bonded inks he studied contained copper, cadmium, and bismuth as the binder additives. He further studied two pastes he made himself - one from CuO and one from CdO - which contained no gold or other inorganic material.

All were printed and fired onto Coors 96-wt pct alumina, which he characterized as containing ∿4-wt pct silica and minor amounts of Ca, K, Na, and Mg. The films were fired in a belt furnace at a series of temperatures from 850 to 1050°C with 15-min dwell at peak temperature.

Analysis of the binder phases and interfaces was accomplished by use of the following techniques: selective etching, with aqua regia or nitric acid to remove gold, glass, and metal oxides or with a KI-I_2 etchant solution which removed only gold; determination of the weight gain of fired specimen substrates after printing, firing, and etching; determination of the adhesion strength of unetched films; x-ray diffraction of etched film surfaces; SEMography; and EDAX analysis of features detected in the SEM. Table 3 (see p. 23) details some of the more important thesis findings.

5. R. J. Lisauskas, "Characterization of the Reaction between Thick-Film Reactive-Bonded Gold Pastes and Alumina Substrates," Master's Thesis, Massachusetts Institute of Technology, June 1976.

The conclusions Lisauskas drew from his work are summarized below.*

A. At 1100°C the CuO paste and alumina substrate react to form the spinel $CuAl_2O_4$. No $CuAlO_2$ was detected, in agreement with the phase diagram of Jacob and Alcock shown in Fig. 25 [6]** and a model according to which spinel formation occurs at the $CuAl_2O_4$-Al_2O_3 phase boundary.

B. The pastes of CuO and CdO react with the substrate to form $CuAl_2O_4$ and $CdAl_2O_4$ (also a spinel), respectively. The amount formed is a thermally activated function of the firing temperature, which ranged from 850 to 1050°C.

C. The activation energies for spinel formation from the CdO and CuO pastes agree in general with the activation energies for M^{2+} ion diffusion through MAl_2O_4 spinels determined by galvanic cell experiments. The same mechanism is suggested to limit spinel formation from the CdO and the CuO pastes.

D. Reactively bonded thick-film gold pastes based on a 3Cu:1Cd binder wt ratio form a spinel at the substrate interface. The fit to an Arrhenius relationship is not as good as that for the CdO and CuO pastes, but the slopes and the activation energies of spinel formation for the two reactively bonded inks are clearly different from those of the metal oxide pastes. The rate-limiting mechanism for spinel formation is judged to be different from that in the case of the metal oxide pastes.

---

*In this summary the wording of Lisauskas's conclusions has been changed to restate them in the terminology we have used throughout the contract study and to condense them.

**The phase diagrams of Misra and Chaklader [7] and Gadalla and White [8] also describe the system. The three disagree on several points.

6. K. T. Jacob and C. B. Alcock, "Thermodynamics of $CuAlO_2$ and $CuAl_2O_4$ and Phase Equilibria in the System Cu_2O-CuO-Al_2O_3," J. Am. Ceram. Soc. 58, 192 (1975).
7. S. K. Misra and A. C. D. Chaklader, "The System Copper Oxide-Alumina," J. Am. Ceram. Soc. 46, 509 (1963).
8. A. Gadalla and J. White, "Equilibrium Relationships in the System CuO-Cu_2O-Al_2O_3," J. Brit. Ceram. Soc. 63(1), 39 (1964).

TABLE 3. SUMMARY OF EXPERIMENTAL FINDINGS

Paste, Type, Composition of Additives to Gold	Adhesion Behavior	Thermally Activated Growth of Spinel at the Interface (grams). (Data normalized to wt at 850°C.)	Total Weight of Spinel and Metal Oxide Interfacial Materials	SEMogra after and Me Stated
CuO paste	N/A*	$W_{int}^{**} = 2 \times 10^{11} e^{\frac{-87 \text{ kcal/mole}}{RT}}$ Correlation factor was 99 pct for firing temps. from 900 to 1050°C.	N/A	Identi irregul ∿1- to larger surface ∿80-pc surface 1050°C
CdO paste	N/A	$W_{int} = 3 \times 10^{7} e^{\frac{-62 \text{ kcal/mole}}{RT}}$ Correlation factor was 99 pct for firing temps. from 900 to 1050°C.	N/A	
Au paste No, 1, reactively bonded - 1.8 wt pct Cu 0.55 wt pct Cd	Nominally linear increase with firing temperature from 1 lb† at 900°C to 14 lb at 1015°C.	$W_{int} = 1 \times 10^{5} e^{\frac{-49 \text{ kcal/mole}}{RT}}$ Correlation factor was 98 pct for firing temps. from 900 to 1015°C.	Not measured.	∿80-pc by a p spinel. than Cd samples
Au paste No. 2, reactively bonded - 0.79 wt pct Cu 0.23 wt pct Cd	Nominally linear increase with firing temperature from 1.8 lb at 900°C to 9.5 lb at 1025°C.	$W_{int} = 1 \times 10^{5} e^{\frac{-48 \text{ kcal/mole}}{RT}}$ Correlation factor was 87 pct for firing temps. from 900 to 1025°C.	No wt change at 900 to 1025°C.	
Au paste No. 3, mixed bonded - 0.23 wt pct Cu 1.43 wt pct Cd	Approximately constant at 9.5 lb with firings between 900 and 1025°C.	$W_{int} = 1 \times 10^{10} e^{\frac{-77 \text{ kcal/mole}}{RT}}$ Correlation factor was 99 pct for firings from 900 to 1025°C.	∿ constant wt at 900 to 1000°C (strong increase over 850°C value; decreases from 1000 to 1025°C).	Failed when te not etc
Au paste No. 4, mixed bonded - 0.52 wt pct Cu 0.61 wt pct Cd 0.70 wt pct Bi 0.20 wt pct Ag	Approximately constant at 7.5 lb with firings between 900 and 1025°C.	$W_{int} = 1 \times 10^{10} e^{\frac{-78 \text{ kcal/mole}}{RT}}$ Correlation factor not given. Firing temps. 900-1050°C.	∿ constant wt at 950 to 1025°C (strong increase over 850°C value).	Failed After a look si paste N

*N/A - Not applicable.
**W_{int} - Weight gain of interfacial compounds.
†lb - The strengths of the films expressed in psi in the thesis are shown here as failure load for a $(0.08\text{-in.})^2$ pad, by multiplying Lisauskas's stress value by his pad areas.
††d_{220} - The lattice spacing between adjacent planes of Miller index 220.

EXPERIMENTAL FINDINGS IN LISAUSKAS'S THESIS

t of Spinel and Interfacial	SEMographic Data - after Etch Removal of Au and Metal Oxides unless Otherwise Stated	EDAX Analytical Data	x-Ray Diffraction Data
N/A	Identification of new phase growing irregularly on alumina. Particles ∿1- to 2-μm diam after 975°C firing; larger after 1050°C firing but surface coverage only ∿30 pct.		Spinel identified, d_{220} †† = 2.86 Å for 1050°C sample, 2.846 Å for ASTM standard, and 2.84 Å for standard prepared by Lisauskas.
N/A	∿80-pct coverage of alumina surface by a second new phase after 1050°C firing.	New phase contains only Cd and Al, i.e., no glass present.	Spinel identified, d_{220} = 2.88 Å for 1050°C sample (2.86 Å calculated). x-Ray peak intensities less than with CdO-based material. No glass present.
d.	∿80-pct coverage of alumina surface by a phase identified as mixed spinel. Different appearance than CdO or CuO paste samples.	Cu and Cd in spinel particles.	Spinel identified, d_{220} = 2.86 Å; unreacted CuO identified.
e at 900 to			Spinel identified, d_{220} = 2.86 Å.
wt at °C (strong in- 850°C value; rom 1000 to	Failed at glass-gold interface when tested. (Failure surface not etched.)	Spinel phase contains Cd and Cu but no Bi.	Spinel identified, d_{220} = 2.86 Å.
wt at 950 to ong increase value).	Failed at glass-gold interface. After aqua regia etching, samples look similar to those of gold paste No. 3 after etching.		Spinel identified, d_{220} = 2.86 Å.

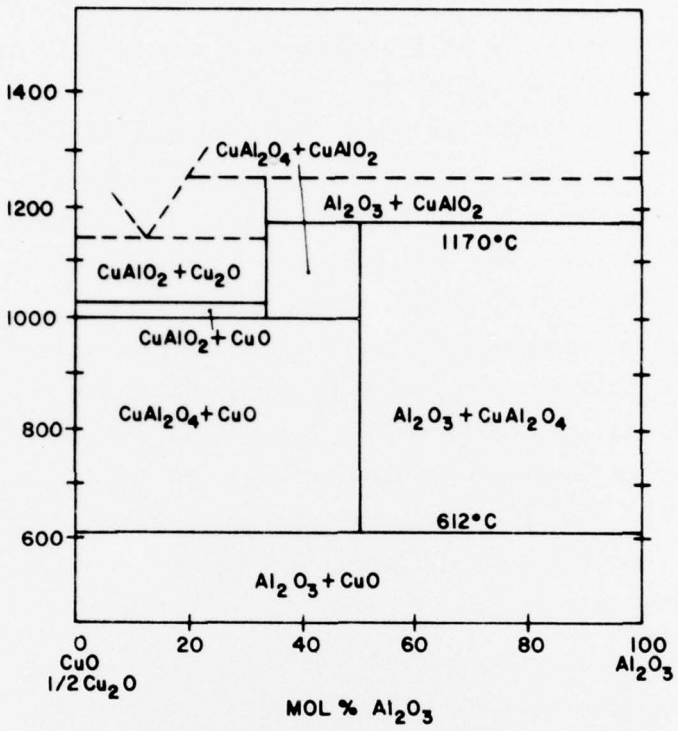

Figure 25. The phase diagram CuO–Al_2O_3 after Jacob and Alcock [6].

E. The spinel which formed for the reactively bonded inks consists of both $CuAl_2O_4$ and $CdAl_2O_4$. Lisauskas could not determine whether the spinel was an intimate mixture of crystallites of each or a partially substituted spinel of the form $Cu_xCd_{1-x}Al_2O_4$.

F. For the reactively bonded gold pastes, a layer of metal oxide was found between the gold and the spinel on the substrates. The gold adheres to the oxide. The layer structure consists of alumina, spinel, metal oxide, and gold containing minor amounts of dissolved copper.

G. For the reactively bonded inks, higher adhesion strengths are obtained with higher firing temperatures. Adhesion is a direct function of the amount of spinel at the interface, an amount that increases with the firing temperature.

H. The character of the Bi_2O_3-containing mixed-bonded inks is different from that of the reactively bonded materials. The amount of spinel in the mixed-bonded films increased with the firing temperature, but the amount of glassy phase, and therefore the adhesion strength, remained nearly constant for firing temperatures from 900 to 1025°C.

I. For Bi_2O_3-containing mixed-bonded films, the interface structure consists of a nearly continuous glassy layer, which covers the spinel and the substrate. The gold adheres principally to the glassy surface and peels away from it during adhesion testing.

J. Reactively and mixed-bonded inks require different firing processes. The required firing process can be predicted if the binder system is known. Reactively bonded inks such as those which Lisauskas studied required higher-temperature firing, e.g., at 1000°C. Mixed-bonded inks are less firing-temperature sensitive; Lisauskas claimed his materials can be fired from 900 to 1025°C without significant changes in the adhesion strength.

In some of these conclusions, particularly J and parts of G and H, Lisauskas has restated RCA findings in terms of the materials he studied. Concerning certain points in the conclusions and other statements of the thesis, the RCA study team would prefer an alternative interpretation of the results. In general, however, Lisauskas's experimental findings agree with our findings, and can be reconciled in the few places where they do not.

SECTION IV

DISCUSSION

Lisauskas has clearly proven that CdO and CuO can react with 96 wt pct Al_2O_3 substrate surfaces to form spinel(s) by one or more thermally activated mechanisms. It is also clear that in reactively bonded ink films the adhesion strength increases along with the amount of spinel for firings of increasing temperature. On the other hand, we believe that Lisauskas's contention that the gold film in reactively bonded inks adheres principally to a metal oxide layer which in turn adheres to the spinel has not been proven satisfactorily. In earlier work we had found, but not identified, a layer which appeared loosely adherent on more poorly adherent firings of reactively bonded film by SEMography of specimens after mercury-vapor leaching. Compare Ref. [1], Fig. 23, and Ref. [5], Fig. 15. Mercury-vapor leaching should not attack cadmium or copper oxides, although it could lift them free of the substrate if the mercury condensed rapidly under the metal oxide layer. Thus mercury-vapor leaching, used with the low mercury-vapor flux rates we have normally used should reveal approximately the same structures as Lisauskas's KI-I_2 etch. When strongly adherent, reactively bonded thick films have been mercury-vapor leached at RCA, structures that we and Lisauskas regard as spinels have been revealed, but no metal oxide films are usually seen. Compare Ref. [1], Figs. 21 and 26, with Fig. 9 from Lisauskas [5].

Whether the gold adheres principally to spinel or to a metal oxide layer in reactively bonded inks is an important question. There is substantial evidence that the gold sticks preferentially to the spinel in the SEMographs reviewed above and in the following argument: Because Lisauskas normalized all his weight gain data to his 850°C samples, it is not possible for the reader to obtain an accurate picture of how the weight of metal oxide decreased in the high-temperature-fired, reactively bonded samples. It is, however, clear that it did decrease since the normalized weight of binder additive (CuO and CdO as oxides or combined into spinel) remained constant at the gold-ceramic interface for increasing firing temperatures, and since the amount in spinel form increased. Thus the reduction in the amount of metal oxides in the interface correlates directly with the increase in adhesion strength.

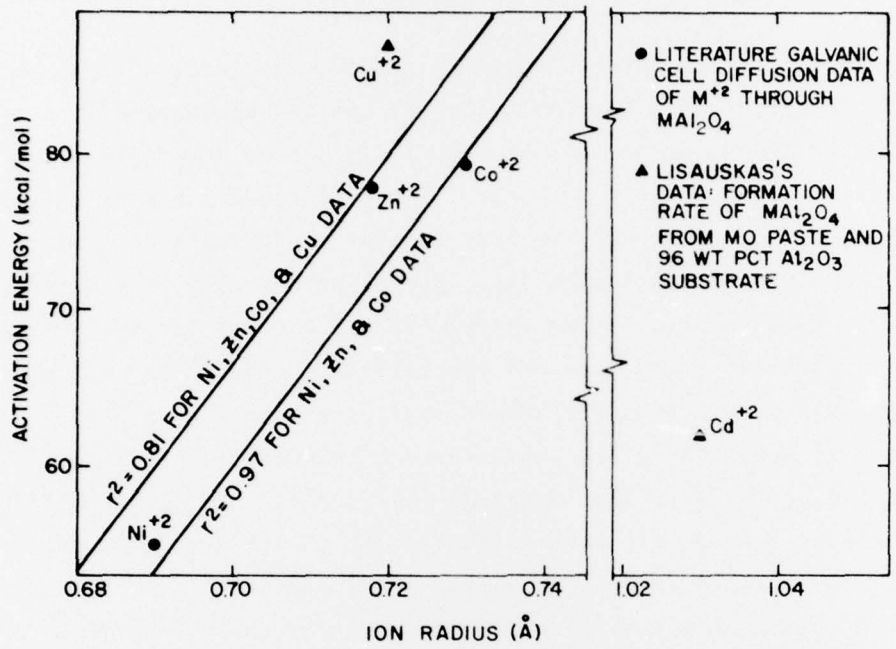

Figure 26. Comparison of the activation energies for spinel formation with the divalent cation radii.

Even if some metal oxide is always present at the interface, the principal adhesion mechanism could still be adhesion of the gold to the spinel through holes in the oxide. Delineation of this point will be a principal object of continued experiments.

The activation energy data for spinel formation shown in Table 3 have been explained only in the case of the copper paste ink. Conclusion C was made on the basis of a moderately good fit* of the ionic radius of Cu^{2+} and the activation energy for the formation of $CuAl_2O_4$ with a series of data pairs for the ionic radii of Ni^{2+}, Zn^{2+}, and Co^{2+}, and the activation energies for the diffusion of these ions through their respective spinels. The point for cadmium does not fit at all with the rest of the data, as shown in Fig. 27.

*The coefficient of determination, r^2, of the straight line calculated by a least-squares fit of the data was reduced substantially by the addition of the copper data point, as shown in Fig. 26.

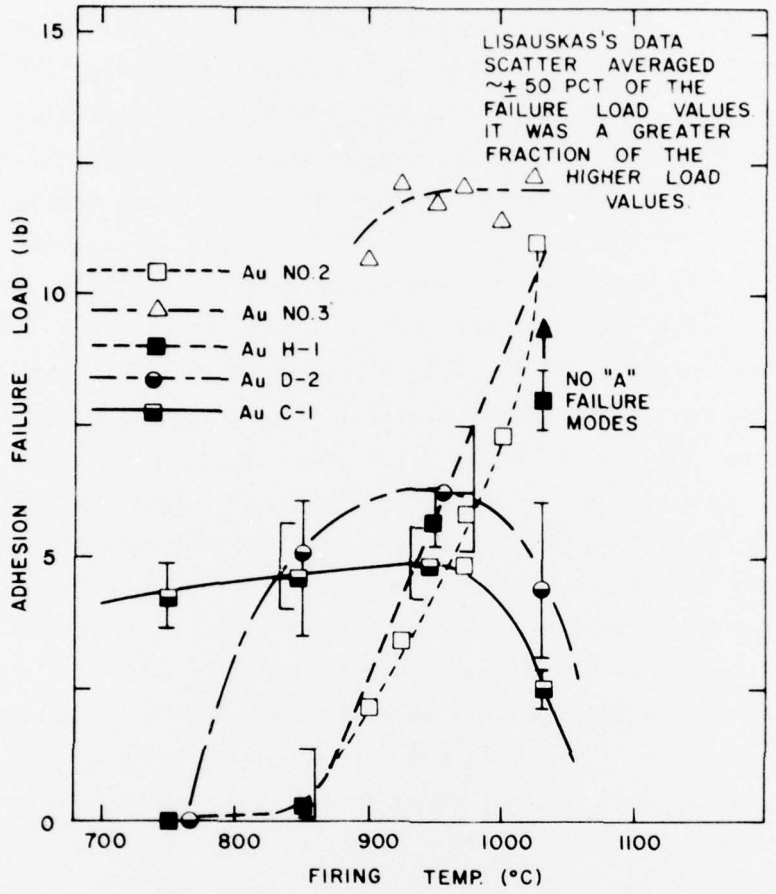

Figure 27. The adhesion strength of reactively bonded and mixed-bonded gold conductors as a function of firing temperature.

Hence Conclusion C has validity only for the formation of $CuAl_2O_4$. Available diffusivity data and pertinent theories are under study to achieve a better understanding of the kinetics of interfacial phase formation in these systems.

For the reactively bonded gold inks, surface, interfacial, grain boundary, or bulk atomic diffusion models may prove useful. The presence of a metal oxide layer could have influence on the kinetics of spinel formation. A surface diffusion model for the spread of CdO over Al_2O_3 to form spinel may be required to explain this phenomenon, but data on $CdAl_2O_4$ formation have not proved readily available. It has not been possible even to find a phase diagram for the system $CdO-Al_2O_3$.

Several comments are appropriate concerning Lisauskas's mixed-bonded ink studies. With these materials Lisauskas found a strongly different activation energy for spinel formation from that of the reactively bonded inks. A liquid phase may be present during the firing of these inks. A review of the applicable phase diagrams noted in the Appendix - particularly Bi_2O_3-CuO and Al_2O_3-Bi_2O_3 - strongly indicates that a liquid phase must form. Material transport should be strongly influenced by the presence of a liquid phase. The amount of the liquid phase, its solubility for CuO, CdO, and Al_2O_3, and its viscosity as a function of temperature would be critical properties of the liquid. The time during which the limited amount of Bi_2O_3 could dissolve other species before solidifying, the chemical species it deposits during solidification, the location of such deposits, and the way the molten frit phase might be absorbed into a porous substrate could also strongly affect the kinetics of spinel formation.

The part of Conclusion H which states that the adhesion strength of the mixed-bonded inks remains essentially constant is based on adhesion strength data containing a great deal of scatter. Figure 27 compares the data from two of Lisauskas's reactively bonded and mixed-bonded gold inks with that from similar materials taken by RCA. The compositions of all of Lisauskas's inks and the compositions of the RCA-studied inks are shown in Table 4.

To compare such adhesion data taken in two different laboratories is tenuous, since the soldered-wire tensile peel test is known to be sensitive to the assembly techniques and handling of test specimens. RCA has, however, recently developed the test to a high degree of precision [9]. To plot Lisauskas's data, which report his failure strengths as load per unit area, for comparison with RCA's data, we chose to normalize the data. Lisauskas

9. T. T. Hitch, "Reproducible Adhesion Test for Soldered Thick-Film Conductors," Final Report on Naval Avionics Facility Indianapolis Contract No. N00163-76-C-0287, to be released approximately Sept. 1977.

TABLE 4. THE COMPOSITIONS OF THE BINDER PHASES OF INK MATERIALS STUDIED BY LISAUSKAS AND BY RCA

Gold Ink Designation	Binder Type	Binder Composition (wt pct)*						
		CuO	CdO	Bi_2O_3	ZnO	PbO	SiO_2	B_2O_3
RCA [1] Code H-1	Reactively bonded	0.88	0.23					
RCA [1] Code D-2	Mixed-bonded	0.25	0.93	2.0				
RCA [1] Code C-1	Mixed-bonded	0.5			1.0	2.5	0.2	0.5
Lisauskas No. 1	Reactively bonded	2.25	0.63					
Lisauskas No. 2	Reactively bonded	0.99	0.26					
Lisauskas No. 3	Mixed-bonded	0.29	1.63	1.23				
Lisauskas No. 4	Mixed-bonded	0.65	0.69	0.78				

*The binder compositions have all been calculated as if they were present as the most likely oxide at 1000°C. The compositions are expressed as wt pct of the total inorganic material in the inks.

most probably obtained each of his failure stress values, S, in psi values according to the standard formula

$$S = \frac{F}{A} \tag{1}$$

where F is the failure load in lb and A is the test-pad area $(0.080 \text{ in.})^2$.

The soon-to-be-released study of this test method [9] indicates that a linear dependence of the failure load with test-pad width holds in such tests. Accordingly, we converted Lisauskas's data to the failure load values shown in Table 3 and have further normalized them in Fig. 27 to be comparable to our data that were taken with $(0.10\text{-in.})^2$ metallized test pads. The following conversion was used to normalize Lisauskas's data for Fig. 27:

$$\begin{aligned} F \text{ plotted} &= \left[S(\text{psi})\right] \times \left[0.08 \text{ in.}\right]^2 \times \left[\frac{0.10 \text{ in.}}{0.08 \text{ in.}}\right] \\ &= \left[S \times 0.008\right] \text{ (lb)} \end{aligned} \tag{2}$$

The good agreement of data between the two similar reactively bonded inks, H-1 and No. 2 in Fig. 27, gives credence to the comparison. Furthermore, except for the test-pad areas, the tests run by both groups were similar. The solder was 12In-70Sn-18Pb (in wt pct), and the Instron loading rate was 0.5 in./min in test procedures. The difference in wire diameters - 0.032 in. for RCA and 0.022 in. for Lisauskas - should not affect the data significantly so long as "A" failure modes are observed [9].

An "A" or adhesive failure mode is one in which the pad solder and wire are pulled clearly off the substrate during testing. Lisauskas does not describe his failure modes in detail but does mention a transition to non-"A" failure modes for the higher-strength reactively and mixed-bonded films. His constant failure load data may be the result of a failure mode that no longer reflects the film-to-substrate adhesion strength, but instead shows the strength of the solder, the wire, or the bulk gold film.

On the basis of our study of the data, we believe it is not advisable to conclude adhesion strengths of mixed-bonded inks are constant with firing temperature. However, a conclusion that there is a reduced sensitivity to firing

temperature in the mixed-bonded inks compared with reactively bonded inks may certainly be drawn from Lisauskas's data and is in agreement with our data. Why Lisauskas's adhesion strengths for his mixed-bonded Au ink No. 3 is much higher than our data for ink D-2 is not known.

Conclusion I indicates that the Bi_2O_3 glassy phase covers the spinel and that the adhesion of the gold is principally to the glassy layer. The gold may be adhering to the spinel through holes in the Bi_2O_3 frit. This appears possible from Lisauskas's and RCA's SEMographs and from our Auger studies, but more study will be necessary to define the adhesion mechanism in mixed-bonded systems.

Lisauskas did not report $MgAl_2O_4$ on the surface of his as-received substrates. Analysis by x-ray diffraction of the surfaces of Coors ADS96F substrates (and a great many other 96 and 99.5 wt pct alumina substrate surfaces*) indicates that most contain significant amounts of $MgAl_2O_4$ spinel. Moreover, instead of the minor impurity Lisauskas states it to be, MgO was present in our ADS96F at ∿1.0 wt pct, i.e., ∿25 pct of the binder-phase additions to the alumina. Indeed, Lisauskas's EDAX surface analyses of the substrate indicated the presence of magnesium despite its low atomic number.

It appears unlikely that the isomorphic spinels $MgAl_2O_4$, $CdAl_2O_4$, and $CuAl_2O_4$, each with a lattice parameter within one percent of the others, would occupy the same surface with complete independence. Accordingly, the possibilities of epitaxial growth of copper and cadmium spinels on $MgAl_2O_4$ and of the formation of three cation spinel mixtures, e.g., $Cu_xCd_yMg_{1-x-y}Al_2O_4$, must be considered.

*Private communication, Dr. Eric Hockings, RCA Laboratories, July 1977.

SECTION V

FUTURE WORK

Further investigation of sintering kinetics are necessary at a lower temperature to determine the influence of glass content on densification. At some temperature near the glass softening point, i.e., 485°C, the glass may not be sufficiently fluid to be useful in the primary and secondary sintering stages.

An additional factor which could influence low-temperature sintering is the polymer burn-off behavior. Normal thick-film inks contain a small amount of polymer, e.g., ethylcellulose, to enhance the strength of the film prior to sintering. If traces of the polymer are still volatilizing while the metal phase is sintering, some gas entrapment might result with a subsequent loss in metal densification.

Therefore, both low-temperature glass properties and polymer characteristics may have a considerable effect on pore size and distribution in the sintered metal network. These factors may ultimately affect the microstructure which is produced in the metal when it finally reaches the higher sintering temperatures.

With regard to the mixed- and reactively bonded conductors, it would be helpful to determine whether the spinel phases are mixtures of magnesium, copper, and cadmium spinels or are partially substituted spinels of the form $Cu_xCd_yMg_{1-x-y}Al_2O_4$. Experiments to make this distinction will be sought. Simple x-ray diffraction techniques do not appear to have sufficient resolution.

As a part of the effort, a study of epitaxial growth of $CdAl_2O_4$ and $CuAl_2O_4$ spinels on $MgAl_2O_4$ will be made by use of a variety of analytical tools. Discussions with NRL scientists have suggested that x-ray photoelectron spectroscopy (XPS) may be the analytical tool of choice, since it has a better lateral resolution than Auger spectrometry and a better sensitivity than EDAX for elements in the surface atom layers of a specimen. It is likely that a combination of NRL and RCA analytical techniques and talents will be employed to answer the question of spinel epitaxy.

Some of the questions concerning reaction rate, introduced but left unanswered by Lisauskas, were mentioned in the Discussion (Section IV). A phase-diagram study on the CdO-Al_2O_3 system would be beneficial to an understanding

of the kinetics of these reactions. Selected experiments in the CdO-CuO-Al_2O_3 system, with and without Bi_2O_3 additions, are expected to be valuable. Experiments using Lisauskas's KI-I_2 and aqua regia etches and comparisons of these etchants with mercury-vapor leaching are expected to be informative.

The critical question of whether the gold film sticks to metal oxide or to spinel in reactively bonded inks and to a CuO-loaded Bi_2O_3 frit phase or to spinel in the mixed-bonded inks must be determined. Plans for critical experiments in these areas are underway. A closely related area, which Lisauskas did not address, is the reduction of adhesion strength in mixed-bonded inks by overfiring. The manner in which the interface changes has been studied only briefly (by means of Auger spectrometry at RCA [2]). Further work in this area is required.

APPENDIX

The reactions between the various phases of inks and ceramics in thick-film materials are complex. Some insight into these reactions can be gained by studying the phase diagrams for some of the phases, where they have been described. The following is a short list of some reactions which it is believed may be important to thick films and their adhesion. The information is taken from a set of compilations of such information [10-12].

Reactants	Reaction Data	Ref.	Fig. No.
Al_2O_3-Bi_2O_3	Eutectic at 97 mol pct Bi_2O_3 and 820°C. Liquidus at 93 mol pct Bi_2O_3 and 1070°C.	12	4365
Al_2O_3-MgO-SiO_2	For a 96 wt pct substrate with 3 pct SiO_2 and 1 pct MgO, cordierite is not as likely to occur as are sapphirine, corundum, or spinel.	11	2535
Al_2O_3-CdO	$CdAl_2O_4$ was found to be rhombohedral. The spinel form was not observed.	12	4318
Bi_2O_3-CdO	Eutectic at 17 mol pct Bi_2O_3 and ∿795°C.	10	326
Bi_2O_3-PbO	Eutectic at ∿25 mol pct Bi_2O_3 and ∿730°C.	10	326
Bi_2O_3-CuO	Eutectic at 90 mol pct Bi_2O_3 and ∿600°C.	12	4178
CuO-SiO_2	Eutectic at 8 wt pct SiO_2 and 1050°C.	11	2142
CuO-Al_2O_3	Phase diagrams by Misra and Chaklader [6] and by Gadalla and White [7] are shown.	11	2085-2094
PbO-SiO_2	Several eutectics at high PbO concentrations and ∿720°C.	10	284

10. E. M. Levin et al., *Phase Diagrams for Ceramists*, The American Ceramic Society, Columbus (1964).
11. E. M. Levin et al., *Phase Diagrams for Ceramists 1969 Supplement*, The American Ceramic Society, Columbus (1969).
12. E. M. Levin and H. F. McMurdie, *Phase Diagrams for Ceramists 1975 Supplement*, The American Ceramic Society, Columbus (1975).

REFERENCES

1. T. T. Hitch and K. R. Bube, "Basic Adhesion Mechanisms in Thick and Thin Films," Final Report, NASC Contract No. N00019-C-74-0270, 31 January 1975.

2. T. T. Hitch and K. R. Bube, "Basic Adhesion Mechanisms in Thick and Thin Films," Final Report, NASC Contract No. N00019-75-C-0145, 30 January 1976.

3. K. R. Bube and T. T. Hitch, "Basic Adhesion Mechanisms in Thick and Thin Films," Final Report, NASC Contract No. N00019-76-C-0256, 31 January 1977.

4. T. T. Hitch and K. R. Bube, "Basic Adhesion Mechanisms in Thick and Thin Films," Quarterly Technical Report No. 1, NASC Contract No. N00019-77-C-0176, 30 April 1977.

5. R. J. Lisauskas, "Characterization of the Reaction between Thick-Film Reactive-Bonded Gold Pastes and Alumina Substrates," Master's Thesis, Massachusetts Institute of Technology, June 1976.

6. K. T. Jacob and C. B. Alcock, "Thermodynamics of $CuAlO_2$ and $CuAl_2O_4$ and Phase Equilibria in the System Cu_2O-CuO-Al_2O_3," J. Am. Ceram. Soc. 58, 192 (1975).

7. S. K. Misra and A. C. D. Chaklader, "The System Copper Oxide-Alumina," J. Am. Ceram. Soc. 46, 509 (1963).

8. A. Gadella and J. White, "Equilibrium Relationships in the System CuO-Cu_2O-Al_2O_3," J. Brit. Ceram. Soc. 63(1), 39 (1964).

9. T. T. Hitch, "Reproducible Adhesion Test for Soldered Thick-Film Conductors," Final Report on Naval Avionics Facility Indianapolis Contract No. N000163-76-C-0287, to be released approximately Sept. 1977.

10. E. M. Levin et al., *Phase Diagrams for Ceramists*, The American Ceramic Society, Columbus (1964).

11. E. M. Levin et al., *Phase Diagrams for Ceramists 1969 Supplement*, The American Ceramic Society, Columbus (1969).

12. E. M. Levin and H. F. McMurdie, *Phase Diagrams for Ceramists 1975 Supplement*, The American Ceramic Society, Columbus (1975).